

## Biological Systems as Nanoreactors: Anomalous Small-Angle Scattering Study of the CdS Nanoparticle Formation in Multilamellar Vesicles

Attila Bóta,<sup>\*,†</sup> Zoltán Varga,<sup>†</sup> and Günter Goerigk<sup>‡</sup>

*Institute of Physical Chemistry, Budapest University of Technology and Economics, Műegyetem rkp 3, H-1521 Budapest, Hungary, and Institute of Solid State Physics, Research Centre Jülich, D-52425 Jülich, Germany*

*Received: November 22, 2006; In Final Form: January 15, 2007*

The formation of cadmium sulfide (CdS) particles in the gaps between the layers of the multilamellar vesicles is described, introducing a new pathway in the preparation of nanometer-scale particles. The in situ structural characterization of both the CdS particles and the vesicles as a reaction medium was performed in the early and final states of the process by using anomalous small-angle X-ray scattering (ASAXS) and freeze-fracture methods. The ASAXS method provides the separation of the scattering of nanoparticles present in a small amount, whereby the monitoring of their formation and growth in the whole time range of manufacturing has become possible.

### Introduction

In the last decades, significant research interest has turned to nanoparticles due to their unusual properties that can be employed in a great number of applications.<sup>1–3</sup> Among the different nanometer-scale particles, the preparation and the characterization of the semiconductor particles represent an important field as a consequence of their potential utilization in nonlinear optics, photocatalysis, and photodegradation.<sup>4–6</sup> Several methods provide the in situ synthesis of these particles using reverse micelles, Langmuir–Blodgett films, clay minerals, microemulsions, polyelectrolyte/surfactant complexes, ordered polypeptide or other organic matrixes, hydrated derivatives of polysaccharide prepared from bacteria, vesicles, and very recently multiwalled carbon nanotubes as reaction mediums.<sup>7–16</sup> Due to its optimum characteristics among many semiconductor nanoparticles, cadmium sulfide (CdS) is the most often studied and described. Unilamellar vesicles (or in an other word, liposomes) consisting of natural or artificial amphiphilics are ideal systems for the synthesis of CdS nanoparticles.<sup>17,18</sup> The unilamellar vesicle preparation, however, requires high-purity chemicals and very precise processes to ensure the quality of nanoproductions.

Here, we show that the water shells of multilamellar vesicles may prove to be adequate reaction compartments instead of the aqueous core of the unilamellar vesicle. The multilamellar vesicles are generally used as model systems of biological cell membranes because of their similarities.<sup>19,20</sup> They form spontaneously, and they are thermodynamically stable, while the unilamellar ones are rather metastable. Consequently, the application of the multilamellar vesicles as nanoreactors insures more extended versatility for both the particle size modification and shape modification than that of their unilamellar form.

Especially, the anomalous small-angle X-ray scattering (ASAXS) can provide information about the matrix and at the same time about the formation of the nanoparticles. This method gives the description of local structures induced by different elements, for example, Cd ions.<sup>21,22</sup> The theory of this method is based on the energy dependence of the scattering factors ( $f_{\text{Cd}}$ ) of the type of the resonant atoms:

$$f_{\text{Cd}}(E) = f_{0,\text{Cd}} + f'_{\text{Cd}}(E) + if''_{\text{Cd}}(E) \quad (1)$$

Thus, the scattering amplitude of the system can be divided into an energy-independent term ( $A$ ) and an energy-dependent ( $(f' + if'')V$ ) term. In this case, the total intensity contains three terms as follows:<sup>23,24</sup>

$$I(q, E) = A(q)^2 + 2f'(E)A(q)V(q) + (f'^2(E) + f''^2(E))V(q)^2 \quad (2)$$

The ASAXS study requires measurements at two different energies at least, at an energy close to the absorption edge of cadmium and at another one far away from it. The difference of two ASAXS curves measured at two different energies (known as separated ASAXS curves) is characteristic of the structure of the domains having Cd ions. This separated ASAXS curve, however, contains two terms, the cross-term and the “pure resonant” term, as is described by the next equation:<sup>24,25</sup>

$$\begin{aligned} \Delta I(q, E_1, E_2) &= I(q, E_1) - I(q, E_2) = \\ &= 2(f'(E_1) - f'(E_2))A(q)V(q) + \\ &+ (f'^2(E_1) - f'^2(E_2) + f''^2(E_1) - f''^2(E_2))V^2(q) \quad (3) \end{aligned}$$

\* To whom correspondence should be addressed. Phone: +36 1 463 2473. Fax: +36 1 463 3767. E-mail: abota@mail.bme.hu.

<sup>†</sup> Budapest University of Technology and Economics.

<sup>‡</sup> Research Centre Jülich.

Executing the ASAXS measurements at three different energies, the determination of the pure resonant term (the

scattering of the CdS nanoparticles) is possible by using the next expressions:

$$V_{\text{Cd}}^2(q) = \frac{1}{C(E_1, E_2, E_3)} \left[ \frac{\Delta I(q, E_1, E_2)}{f'(E_1) - f'(E_2)} - \frac{\Delta I(q, E_1, E_3)}{f'(E_3) - f'(E_2)} \right]$$

$$C(E_1, E_2, E_3) = f'(E_2) - f'(E_3) + \frac{f''^2(E_1) - f''^2(E_2)}{f'(E_1) - f'(E_2)} - \frac{f''^2(E_1) - f''^2(E_3)}{f'(E_1) - f'(E_3)} \quad (4)$$

The anomalous method not only gives a qualitative description about the system without any separation technique, but it also provides a quantitative determination of the nanoparticles present in very low concentration with a high statistical significance, providing a precise tool in quantitative chemistry.

### Materials and Methods

The fully hydrated DPPC/water vesicles (20 w/w %) containing Cd<sup>2+</sup> ions were prepared from synthetic high-purity 1,2-dipalmitoyl-*sn*-glycero-3-phosphatidylcholine (DPPC, obtained from Avanti Lipids, AL) and from aqueous Cd(NO<sub>3</sub>)<sub>2</sub> neutral buffer solution (17 mmol/dm<sup>3</sup>, insures a 0.05 Cd<sup>2+</sup>/lipid molar ratio) by simple mixing and by vortex homogenization. Aqueous (NH<sub>4</sub>)<sub>2</sub>S (20 w/w %) was added to the vesicle system (in a 1.2 (NH<sub>4</sub>)<sub>2</sub>S/Cd<sup>2+</sup> molar ratio) then mixed by vortex intensively.

The small-angle X-ray scattering (SAXS) and the anomalous small-angle X-ray scattering (ASAXS) measurements were carried at the JUSIFA facility (Jülich's user-dedicated small-angle scattering facility) at the DORIS synchrotron radiation source in DESY (German Electron Synchrotron, Hamburg).<sup>26</sup> The studies of the vesicles covered a range in real-space resolution on the length scale from 1 up to 50 nm, corresponding to a scattering interval of the scattering variable ( $q$ ) (defined as  $(4\pi/\lambda) \sin \Theta$ , where  $\lambda = 0.464 \text{ \AA}$  is the wavelength of the selected X-ray beam and  $2\Theta$  is the scattering angle) from 0.013 to 0.6 1/Å. The ASAXS curves were detected at 26 711, 26 653, and 26 120 eV in the vicinity of the Cd–K absorption edge (26 711 eV). The intensity is given in absolute units of macroscopic cross section (cm<sup>−1</sup>). The anisotropic scattering patterns were monitored with a two-dimensional position sensitive detector, a multiwire proportional counter (MWPC) with 256 × 256 resolution pixels on a 180 × 180 mm<sup>2</sup> active area.

The freeze-fracture electron microscopy was used for the direct visualization of local structures of vesicles with CdS nanoparticles.<sup>27</sup> The gold sample holders used in freeze fracture were preincubated at 24 °C at the same temperatures as the samples. Droplets of about 1 μL from the samples were pipetted onto the gold holders which were then immediately plunged into liquid-nitrogen-cooled partially solidified Freon for freezing. The fracturing was carried out at −110 °C in a Balzers freeze-fracture device (Balzers AG, Vaduz, Liechtenstein). The freeze-fractured faces were etched for 30 s at −100 °C followed by unidirectional platinum/carbon coating at an angle of 45°. Replicas of the samples were removed by submersion into distilled water and subsequently cleaned with a detergent solution; they were then examined using a JEOL JEM-100 CX II (Japan) electron microscope.

The separation of the CdS nanoparticles was executed after a gentle drying of the vesicle system, and then, it was kept under vacuum. The dry sample was dispersed in chloroform and

centrifuged. The CdS particles suspended in chloroform were placed onto amorphous graphite foil and investigated in a Philips CM20 (200 kV) (Holland) electron microscope.

### Results and Discussion

The fully hydrated DPPC/water vesicles exhibit at least five Bragg rings in their two-dimensional small-angle X-ray scattering (SAXS) pattern corresponding to a well ordered multilamellar and macroscopically not oriented structure formed in the gel phase at 24 °C.<sup>28,29</sup> The divalent metal ions cause significant destructions in the layer arrangement of the multilamellar vesicles indicated by their small-angle X-ray scattering, as the characteristic Bragg reflections of the scattering curve can only be detected in a reduced order number of diffraction.<sup>30–32</sup> This phenomenon occurs if the liposomes contain Cd<sup>2+</sup> ions. The two-dimensional SAXS pattern monitored on the system shows only one diffuse ring, as presented in Figure 1A. The ring extends from 0.06 up to 0.24 1/Å in the scattering variable scale, and it can be interpreted as a sum of the extremely broadened first and second orders of reflection. This character of the SAXS pattern indicates that the lamellarity, the correlation of the bilayers, and the bilayer structure itself are severely destroyed. More detailed information about the location of the Cd ions can only be obtained by means of anomalous scattering.

These ASAXS curves exhibit great similarity, but the closer inspection reveals that their shapes depend on the energy. The closer the X-ray energy is to the cadmium absorption edge, the smaller is the intensity. The difference in the ASAXS curves measured at the two different energies, shown in Figure 1A, is characteristic of the structure of the domains having the Cd ions under investigation. Exactly, this difference provides information about the displacement of the Cd ions. The separated curves are due to the contrast variation resulting from the change in energy, and the shape exhibits an inhomogeneous distribution of Cd ions. It extends up to 5% in the beginning part of the curve and vanishes at a scattering variable of about 0.05 1/Å, indicating the formation of domains rich in Cd ions with a characteristic size in the range of several hundred Å-s. Moreover, the appearance of the diffuse peak in the separated curves indicates that Cd ions are partly located in periodical shell forms corresponding to the diffuse layer arrangement of the destroyed liposomes.

An independent method, the freeze-fracture method, can reveal the defects of the centrosymmetrical lamellar arrangement of the vesicle. In Figure 1B, a vesicle completely broken through is shown and its cross section exhibits a significant irregularity between the lamellae. Some stacks of lamellae are crumpled and gaps are visible between them, which may terminate the long range periodicity, giving an explanation for the diffuse character of the scattering pattern of the system having Cd ions.

Adding (NH<sub>4</sub>)<sub>2</sub>S to the system, the two-dimensional SAXS pattern is drastically changed, as shown in Figure 2A. At least three rings of the Bragg reflections appeared, indicating a significant reconstruction of the ordered vesicle structure. Presumably, the collapse of gaps filled with Cd ions occurs during the formation of compact CdS particles. The position of the first reflection corresponds to a periodicity of 65.1 Å, which is slightly longer than that of the pure DPPC/water system (64.2 Å). The formation of the CdS particles with a cubic crystal structure was confirmed by using wide angle X-ray diffraction in agreement with the reported results.<sup>16</sup> The electron micrograph of a characteristic vesicle is presented in Figure 2B in which we can observe the closely packed parallel layers in the outer leaflets. This is the sign of a rearrangement of a more regular



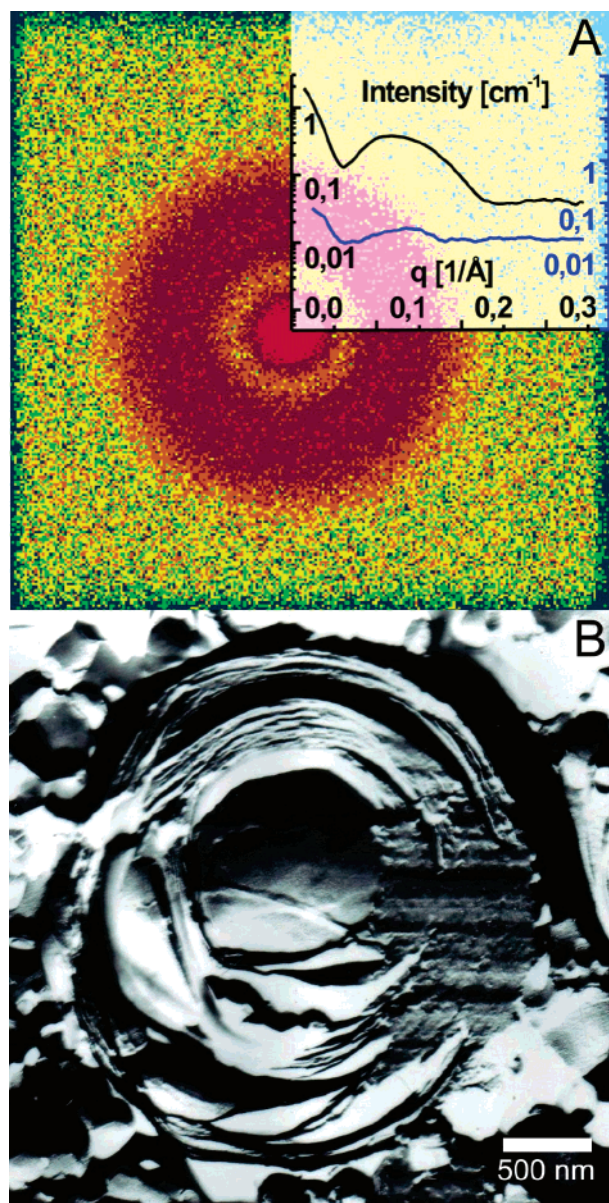


**Figure 1.** (A) Two-dimensional SAXS pattern of the multilamellar dipalmitoylphosphatidylcholine (DPPC)/water vesicles having  $\text{Cd}(\text{NO}_3)_2$  (0.05  $\text{Cd}^{2+}$ /lipid molar ratio, neutral buffer system, measured at 26 120 eV). The broadened single ring is the consequence of a weakly correlated lamellar arrangement. The inset plot shows the shape of this ring in the representation of the one-dimensional scattering intensity vs the scattering variable ( $q$ ). Moreover, the difference of two anomalous small-angle X-ray scattering (ASAXS) curves measured at 26 120 and 26 711 eV is also plotted (blue line). The intense beginning part of this separated form indicates larger domains rich in  $\text{Cd}^{2+}$  ions, and its broadened peak with reduced intensity corresponds to the diffuse character of the layer arrangement of the vesicles. (B) Surface morphology of a giant vesicle broken through, completely. The regular, periodic arrangement of shells is damaged; gaps between the stacks of lamellae appear which are especially visible in the outer leaflets.

layer structure, giving an explanation for the increased number of the Bragg rings. What is even more interesting is that many small grains appear, concentrated locally, in certain layers between the stacks of lamellae. The characteristic size of these particles falls into the range of approximately 5–10 nm. Presumably, these grains are the agglomeration of the CdS nanoparticles. The anomalous scattering provides more structural information about these particles. The ASAXS curves measured at three different energies, plotted in Figure 3A, indicate a trend;

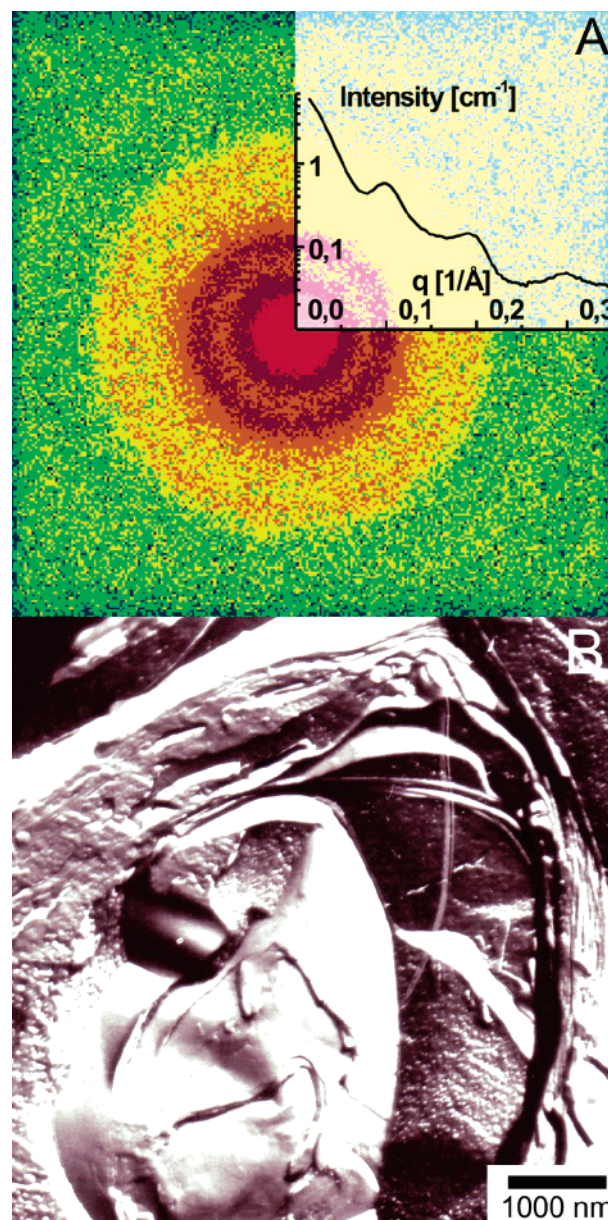


**Figure 2.** (A) Two-dimensional SAXS pattern of the multilamellar DPPC/water vesicles having CdS nanoparticles. The Bragg reflections appearing in three orders are unambiguous signs of the reconstructed multilamellar arrangement. The inset plot exhibits the corresponding one-dimensional scattering intensity vs the scattering variable ( $q$ ). (B) Fractured surface of the inert part of a giant vesicle broken through, completely. Two types of the characteristic morphologies can be recognized; the regular, periodic multilamellar arrangement in the outer leaflets and the great number of CdS nanoparticles embedded between the stacks of lamellae.

the difference in the ASAXS curves diminishes with increasing energy in the first part of the scattering variable range and the differences between them vanish in the scattering variable range of the first Bragg reflection, indicating that the Cd ions are not located in a periodic arrangement of the multilayers. To eliminate the scattering contribution of the vesicles, the measurements were performed at three different energies; thus, we can obtain the pure resonant term, as is described in the Introduction.<sup>33,34</sup> The separated and pure resonant curves exhibit different shapes; the latter diminishes in a narrower range of scattering variables than the former, as is shown in Figure 3B, representing the importance of the determination of the pure

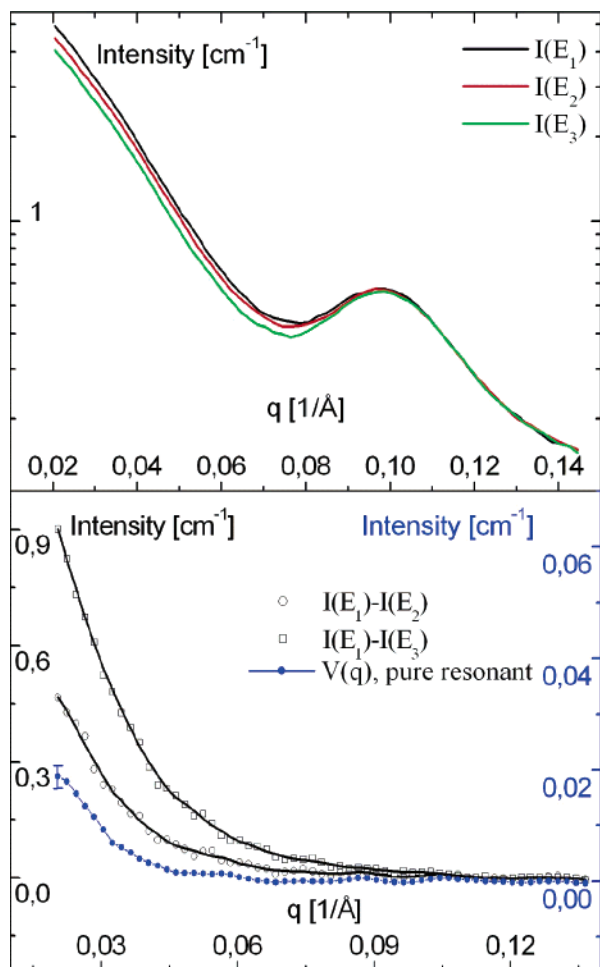


**Figure 3.** (A) ASAXS curves of the DPPC/water vesicles having CdS nanoparticles measured at three different energies ( $E_1 = 26\,120$ ,  $E_2 = 26\,653$ , and  $E_3 = 26\,711$  eV). The curves exhibit reduced intensity as the energy of the X-ray is shifted to the vicinity of the K absorption edge of cadmium. In the range of the first Bragg reflection, the vanished differences between the separated curves indicate the nonperiodic form of the location of the CdS nanoparticles. (B) Separated ASAXS curves measured at  $E_1$ ,  $E_2$  and  $E_1$ ,  $E_3$ , respectively (open circles), and the pure resonant term (filled circles) deduced from these separated forms. The latter curve is strictly characteristic only for the spatial distribution of the  $\text{Cd}^{2+}$  ions of the CdS particles.

resonant term. From this term, a characteristic average diameter of 6.9 nm was derived by assumption of a log-normal size distribution of a spherical form (Figure 4A) corresponding to the next expressions:<sup>25</sup>

$$V_{\text{Cd}}^2(q) = \text{const} \int_0^\infty P(R) \left( \frac{4\pi R^3}{3} \frac{3(\sin(qR) - qR \cos(qR))}{(qR)^3} \right)^2 dR$$

$$P(R) = \frac{1}{\sqrt{2\pi}} \frac{1}{\sigma R} \exp \left[ -\frac{\ln^2 R/R_0}{2\sigma^2} \right] \quad (5)$$

The characteristic size shows a very good agreement with the estimation of the freeze-fracture method. Finally, the CdS nanoparticles were separated from the vesicle system and their size analysis was carried out by using transmission electron microscopy (TEM) (Figure 4B). In the electron micrograph, less spherical but rather squared stocky shaped particles appear and their sizes (6–7 nm) fall exactly into the range of that deduced

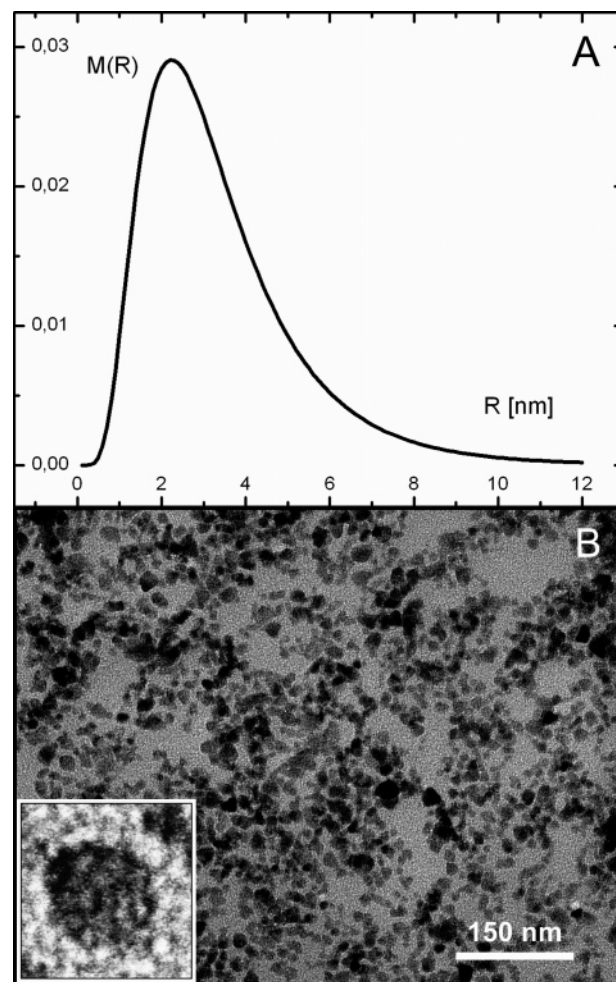


**Figure 4.** (A) Log-normal size distribution of the CdS nanoparticles calculated from the pure resonant term. (B) Typical TEM image of the CdS nanoparticles. The inset (represents a length scale of 10 nm) shows a single CdS nanoparticle.

by the freeze-fracture electron microscopy and more precisely by the ASAXS method.

The application of the ASAXS technique proved to be a useful tool not only to determine but also to follow the formation of nanoparticles during their synthesis. This advantage of the tunable synchrotron radiation may open further new perspectives in nanotechnology.<sup>35</sup> The simultaneous ASAXS studies of the reaction zones of nanoparticles provide an observation and regulation technique of the necessary engineering parameters of synthesis without any separation of the nanoparticles that are present in low concentration in the reaction medium.

**Acknowledgment.** We are grateful to T. Kiss and to Gy. Radnóczy (Research Institute for Technical Physics and Materials Science, Budapest, Hungary) for the electron microscopical investigation of CdS particles. This work was supported by the contract RII3-CT-2004-506008 of the European Community at DESY/HASYLAB (Hamburg, Germany) and by the Hungarian Scientific Funds OTKA (Bóta, T 43055).

## References and Notes

- (1) Valden, M.; Lai, X.; Goodman, D. W. *Science* **1998**, *281*, 1647.
- (2) Huynh, W. U.; Dittmer, J. J.; Alivisatos, A. P. *Science* **2002**, *295*, 2425.
- (3) Bell, A. T. *Science* **2003**, *299*, 1688.



- (4) Colvin, V. L.; Schlamp, M. C.; Alivisatos, A. P. *Nature* **1994**, 370, 354.
- (5) Ramsden, J.; Gratzel, M. *J. Chem. Soc., Faraday Trans. 1* **1984**, 80, 919.
- (6) Mills, A.; Williams, G. *J. Chem. Soc., Faraday Trans. 1* **1989**, 85, 503.
- (7) Fendler, J. H. *Chem. Rev.* **1987**, 87, 877.
- (8) Pileni, M. P.; Motte, L.; Petit, C. *Chem. Mater.* **1992**, 4, 338.
- (9) Zhu, R.; Min, G. W.; Wei, Y. J. *J. Phys. Chem.* **1992**, 96, 8210.
- (10) Dékány, I.; Turi, L.; Tombácz, E.; Fendler, J. H. *Langmuir* **1995**, 11, 2285.
- (11) Caponetti, E.; Pedone, L.; Martino, D. C.; Panto, V.; Liveri, V. T. *Mater. Sci. Eng., C* **2003**, 23, 531.
- (12) Nelson, E. J.; Samulski, E. T. *Mater. Sci. Eng., C* **1995**, 2, 133.
- (13) Pedone, L.; Caponetti, E.; Leone, M.; Militello, V.; Pantó, V.; Polizzi, S.; Saladino, M. L. *J. Colloid Interface Sci.* **2005**, 284, 495.
- (14) Li, Z.; Du, Y. *Mater. Lett.* **2003**, 57, 2480.
- (15) Mann, S.; Hannington, J. P.; Williams, R. J. P. *Nature* **1986**, 324, 565.
- (16) Shi, J.; Quin, Y.; Wu, W.; Li, X.; Guo, Z.-X.; Zhu, D. *Carbon* **2004**, 42, 423.
- (17) Tricot, Y.-M.; Fendler, J. H. *J. Phys. Chem.* **1986**, 90, 3369.
- (18) Korgel, B. A.; Monbouquette, H. G. *Langmuir* **2000**, 16, 3588.
- (19) Cevc, G.; Marsh, D. *Phospholipid Bilayers, Physical Principles and Models*; John Wiley & Sons: New York, 1987.
- (20) Epanand, R.M. *Current topics in Membranes: Lipid Polymorphism and Membrane Properties*; Academic Press: San Diego, CA, 1997.
- (21) Stuhmann, H. B. *Adv. Polym. Sci.* **1985**, 67, 123.
- (22) Guinier, A. *X-Ray Diffraction*; Freeman: San Francisco, CA, 1963.
- (23) de Robbilar, Q.; Guo, X.; Dingenouts, N.; Ballauff, M.; Goerigk, G. *Macromol. Symp.* **2001**, 164, 81.
- (24) Goerigk, G.; Schweins, R.; Huber, K.; Ballauff, M. *Europhys. Lett.* **2004**, 66, 331.
- (25) Varga, Z.; Bóta, A.; Goerigk, G. *J. Phys. Chem. B* **2006**, 110, 11029.
- (26) Haubold, H.-G.; Gruenhagen, K.; Wagener, M.; Jungbluth, H.; Heer, H.; Pfeil, A.; Rongen, H.; Brandenburg, G.; Moeller, R.; Matzerath, R.; Hiller, P.; Halling, H. *Rev. Sci. Instrum.* **1989**, 60, 1943.
- (27) Meyer, H. W.; Richter, W. *Micron* **2001**, 32, 615.
- (28) Wiener, M. C.; Suter, R. M.; Nagle, J. F. *Biophys. J.* **1989**, 53, 315.
- (29) Bóta, A.; Drucker, T.; Kriechbaum, M.; Réz, G.; Pálfi, Zs. *Langmuir* **1999**, 15, 3101.
- (30) Iniko, Y. T.; Yamaguchi, T.; Furuya, K.; Mitsui, T. *Biochim. Biophys. Acta* **1975**, 413, 24.
- (31) Graddick, W. F.; Stamatoff, J. B.; Eisenberger, P.; Bereman, D. W.; Spielberg, N.; *Biochem. Biophys. Res. Commun.* **1979**, 907.
- (32) Bóta, A.; Klumpp, E. *Colloids Surf., A* **2005**, 65, 124.
- (33) Cromer, D. T.; Liberman, D. *J. Chem. Phys.* **1970**, 53, 1891.
- (34) Cromer, D. T.; Liberman, D. *Acta Crystallogr.* **1981**, A37, 267.
- (35) Renaud, G.; Lazzari, R.; Revenant, C.; Barbier, A.; Noblet, M.; Ulrich, O.; Leroy, F.; Jupille, J.; Borensztein, Y.; Henry, C. R.; Deville, J.-P.; Scheurer, F.; Mane-Mane, J.; Fruchart, O. *Science* **2003**, 300, 1416.